

Optimizing Global Flight Altitudes for Contrail Reduction

Insights from Open Flight and Weather Balloon Data

Esther Roosenbrand, Junzi Sun and Jacco Hoekstra
Control and Simulation, Faculty of Aerospace Engineering
Delft University of Technology, The Netherlands

Abstract—As the number of flights increases globally, the aviation industry faces a major challenge of reducing its climate impact. Contrails, besides contributing to global warming by trapping outgoing terrestrial radiation, can potentially offset the benefits of reduced emissions from optimized flight routes.

In this study, we quantify contrail-forming flights on a global scale and evaluate the altitude deviations necessary to avoid contrail-forming regions, using a combination of the Integrated Global Radiosonde Archive (IGRA) data and flight data from OpenSky. The IGRA dataset contains measurements obtained by weather balloons and offers global coverage as well as a high vertical resolution. Mid-Western Europe, Eastern United States of America and Japan were identified as regions with both large volumes of air traffic and a high percentage of these flights forming contrails. These regions are also suitable for altitude changes of less than one kilometer to minimize contrail formation. In addition, regions are identified where a relatively small operational interventions can make a large climate impact.

Keywords—Sustainability, Contrails, Remote Sensing, Atmospheric Science, OpenSky, Aircraft Surveillance Data

I. INTRODUCTION

Currently, global aviation contributes to approximately 5% of net anthropogenic climate forcing [1]. As the number of flights is expected to rise globally, aviation's climate impact will also continue to increase, making sustainability one of the biggest challenges facing the aerospace industry today. Effective sustainability measures, such as alternative fuels and aerodynamic aircraft qui are currently under development. However, their implementation on a commercially relevant scale is expected to take years, perhaps even decades.

Hydrogen power forms a potential solution to aviation's CO₂ emissions, however minimizing the climate impact caused by contrails remains unresolved, even for hydrogen flight. The novel application of multidisciplinary fields beyond aviation alone, such as combining global aircraft surveillance data, atmospheric science, and satellite remote sensing, can help solve this current and future challenge in the form of a climate optimized trajectory model, and can be directly implemented for hydrogen flight as well.

Contrail forming atmospheric conditions are captured by the Schmidt-Appleman criterion (SAC) [2]. SAC is a thermodynamic theory deduced by Schmidt and Appleman and re-examined by Schumann [3], showing that the threshold condition for contrail formation from condensing exhaust water depends on ambient pressure, humidity and the ratio of water and heat released into the exhaust plume. When an aircraft flies through atmospheric conditions that satisfy the

SAC, saturation with respect to liquid water occurs, and a contrail is formed.

Whilst many contrails disappear quickly, persistent contrails have lifetimes of more than five minutes. Persistent contrails occur when the condensing exhaust water does not evaporate (in the given time frame) when mixed with the environment [4]. While persistent contrails are of relevance to our climate-optimized model, non-persistent contrails have a small to negligible climate impact [5], and are thus not relevant for this study. The persistence of a contrail is indicated by the presence of an ice-supersaturation region (ISSR), which forms when the ambient air is supersaturated with respect to ice [3]. Thus for persistent contrail formation, the atmosphere must *both*; satisfy SAC (indicating contrails can theoretically form) *and* fly through an ISSR (indicating they are persistent and thus of relevance to our model).

In practice, avoiding these persistent contrail forming atmospheric regions involves either flying around the perimeter, or flying over or under the region [6]. Typically, due to their broad lateral expansiveness, more environmental benefit is gained if the altitude is varied, rather than rerouted [7]–[9].

A recent paper [10] shows that open source datasets can successfully be used to adequately predict contrail formation. In [10], days and locations with an abundance of contrail formation were identified and analyzed. This skewed dataset does not allow for an accurate indication of the global number of flights producing contrails. Furthermore, the ECMWF (European Centre for Medium-Range Weather Forecasts) data used for atmospheric conditions, has a (comparatively) low vertical resolution of 25 hPa, with interpolation performed between the pressure levels.

The climate optimized trajectory model proposed in our earlier research [11] deviates from a standard wind-optimized route in that it will take into account contrail forming areas, thus minimizing the additional climate impact. However, if the model proposed in [11] were to be implemented, neither the quantitative overall impact nor the scale of the necessary interventions was known at that time. This paper endeavours to quantify the global extent of the contrail forming flights, their geographical location, as well as the typical altitude deviation necessary to avoid contrail forming regions using weather balloon and open flight data.

For all flights within a 50 km buffer around weather balloon station locations, one hour before/after weather balloon releases, it will be determined whether persistent contrails are to be expected, based on SAC and ISSR atmospheric conditions. Subsequently, the number of flights that satisfy

these conditions will be determined, in combination with an analysis of location and season. Contrail formation is highly sensitive to altitude, since ice supersaturated regions (ISSR) are often shallow in height (a few hundreds of meters deep) [6]. Thus, the most straightforward method of contrail-avoidance is altitude deviation, to simply fly outside of the ISSR. With its high vertical resolution, the weather balloon data allows for quantitative estimation of the required deviation.

II. REMOTE SENSING & FLIGHT DATA

This section explains the data sources and the steps taken before further processing to achieve this quantification. In this work, the assessment of the number of flights that fall within an persistent contrail forming atmospheric region and the necessary altitude change required to leave the region, is based on remote sensing and flight data.

A. Integrated Global Radiosonde Archive (IGRA)

The Integrated Global Radiosonde Archive (IGRA) is a collection of radiosonde observations maintained by the National Centers for Environmental Information (NCEI) of the National Oceanic and Atmospheric Administration (NOAA) [12]. Radiosondes are launched daily or twice daily, typically at 0000 and 1200 UTC. During their 1 to 2 hour ascent, at a rate of around 5 meters per second [13], they collect measurements, which are transmitted to ground stations [14].

There, the data is processed into pressure, geopotential height, temperature, relative humidity and derived wind direction and speed from the latitude and longitude of the balloon. Unfortunately not all of the station locations measure the parameter of relative humidity over water vapor, which is necessary to determine the relative humidity over ice. Of the 2788 station locations, only 695 are active in the year of our data analysis 2022, and of these only 304 provide relative humidity measurements. Hence in this paper we use the data collected by the 304 stations.

B. Open flight data: OpenSky

The OpenSky Network has been collecting global air traffic surveillance data since 2013. The unfiltered and raw data is based on ADS-B, Mode S, TCAS and FLARM messages and is open to use [15]. The variables used in this research include: time, latitude, longitude, callsign and the geoaltitude. The spatial coverage of OpenSky is visualized in Fig. 1, with black dots representing station location and the red shading the coverage of each station. The coverage is highest over Europe and North America, whereas due to the nature of terrestrial ADS-B, coverage over the oceans is minimal.

C. Research Area

Around each IGRA station location a 50x50 km² square polygon was drawn. This is deemed to be a reasonable area of influence for a single IGRA measurement, considering the lateral expansive nature of ISSR regions [6]. Subsequently, the locations of OpenSky receivers were overlain with these polygons. If an OpenSky receiver was located within an IGRA polygon, the corresponding IGRA measurement location and OpenSky receiver were used in the research. In Fig. 2.a these

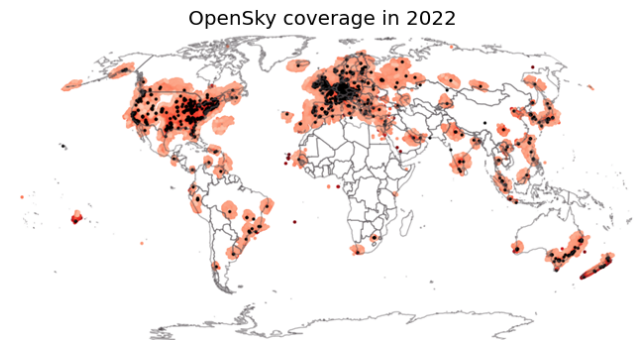
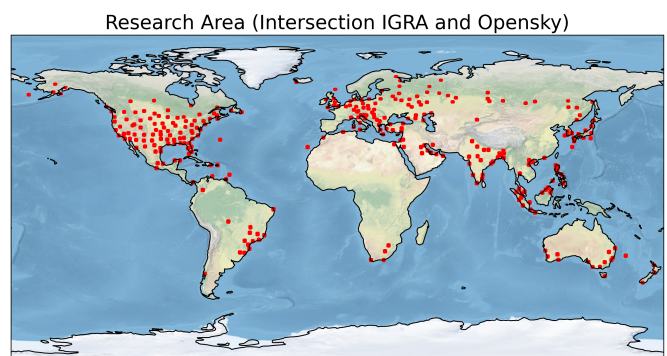
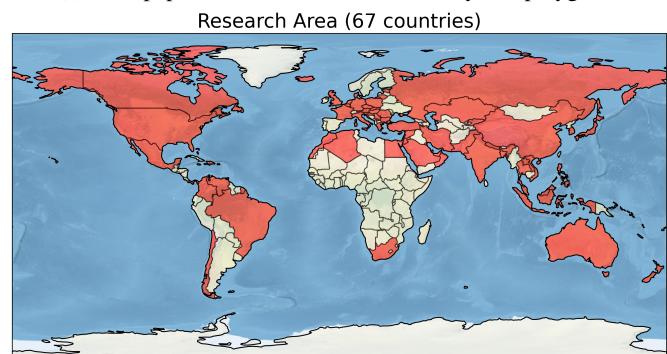


Figure 1: Location of all OpenSky receivers active in 2022 and their coverage across the globe (sourced from: [16]).

overlapping polygons are shown, covering 67 countries as seen in Fig. 2.b.



(a) This paper's research area indicated by red polygons.



(b) Countries featured in this paper's research area

Figure 2: Research Area

III. METHOD

The parameters in the IGRA archives include among others: pressure, geopotential height, temperature and in some cases, relative humidity with respect to water (RH_w). For persistent contrail formation, relative humidity with respect to ice is an essential parameter, any value of RH_w exceeding 100%, indicates the presence of an ISSR. There are numerous ways of converting RH_w to RH_i ; here we use formulas (eq. 1 and 2) by Sonntag [17]. Since the equilibrium vapor pressure of water molecules (e_w) or ice (e_i) depends only

on temperature (T), e can be used to determine the relative humidity with respect to water and ice [18].

$$RH_w = \frac{e}{e_w} \quad (1) \quad RH_i = \frac{e}{e_i} \quad (2)$$

where:

$$\begin{aligned} \log e_w &= -7.90298 \cdot \left(\frac{T_{st}}{T} - 1\right) + 5.02808 \cdot \log\left(\frac{T_{st}}{T}\right) \\ &\quad - 1.3816 \times 10^{-7} \cdot (10^{11.344 \cdot (1-T/T_{st})} - 1) \\ &\quad + 8.1328 \times 10^{-3} \cdot (10^{-3.49149 \cdot (T_{st}/T - 1)} - 1) \\ \log e_i &= -9.09718 \cdot (T_0/T - 1) + 3.56654 \cdot \log(T_0/T) \\ &\quad + 0.876793 \cdot (1 - T/T_0) \end{aligned}$$

with T as the temperature and T_{st} as the steam point temperature (372.15 K).

While $RH_w > 100\%$ does not occur in the Earth's atmosphere, RH_i exceeding 100% is one of the criteria for persistent contrails, and is in fact quite common [17]. Once the relative humidity with respect to ice is obtained, all flights from OpenSky within 50 km buffer around weather balloon station locations, one hour before/after weather balloon releases were downloaded through a OpenSky query. Using the Shapely geometry package [19] in Python, these trajectory lines were intersected with the polygon buffers.

In Fig. 3 an example of a vertical profile of temperature and relative humidity with respect to ice is shown for the Camborne station (UK) on December 12th 2022. In the temperature profile on the left, the vertical blue line indicates the -40°C (233.15 K) SAC condition for contrail formation. The 100% RH_i is shown as a blue line on the right, indicating the ice-supersaturation condition. In addition to the vertical relative humidity profile, aircraft are represented at their respective flight levels. One of the aircraft is indicated in both plots by a red cross (here at an altitude of 11.2 km) satisfies both SAC and the ISSR criterion, thus produces persistent contrails. The two aircraft at higher altitudes (indicated by red dots) satisfy SAC, but not the ISSR criterion, thus should produce non-persistent contrails.

Also illustrated in Fig. 3, is that an altitude increase of a few hundred meters would allow the aircraft indicated by a red cross to drop below the 100% RH_i line, and consequently stop satisfying the ISSR condition and stop producing persistent contrails. This method will be applied to quantify the necessary flight level alterations to minimize contrail formation.

IV. RESULTS

In this section, we first show a general overview of the results, then an examination of both the temporal and geographic effects of contrail formation. After which, we discuss results regarding altitude changes in order to minimize contrail formation. In this paper, it is essential to distinguish between the frequency of the occurrence of atmospheric conditions which produce contrails and the quantity of flights which fly through these atmospheric conditions. If the results show more contrails being produced in the summer months,

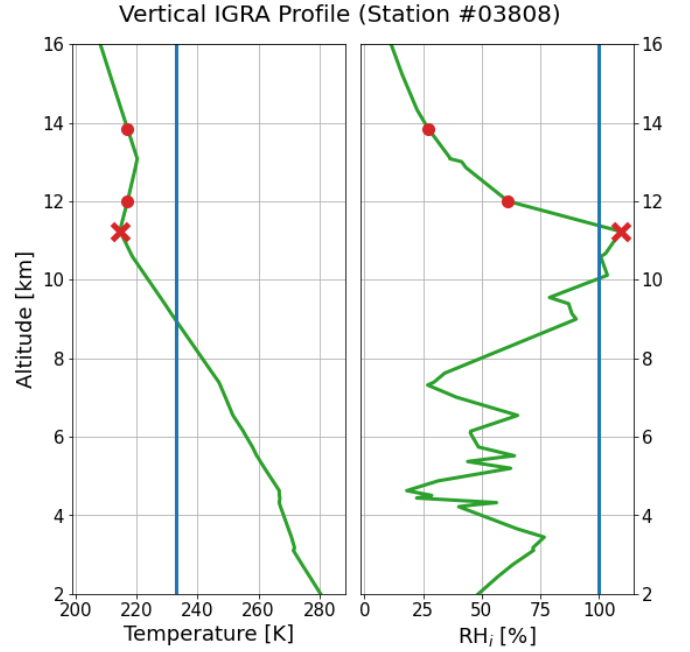


Figure 3: An example of a vertical profile of temperature (left) and relative humidity (right) w.r.t. ice at the Camborne, a U.K. station on Dec 12th 2022 only. One of the aircraft in both plots by a red cross (here at an altitude of 11.2 km) satisfies both SAC and the ISSR criterion, thus produces persistent contrails. The two aircraft at higher altitudes (indicated by red dots) satisfy SAC, but not the ISSR criterion, thus should produce non-persistent contrails.

the question arises if this is because we have more contrail forming atmospheric conditions in the summer, or is this caused by a significant increase of air traffic in summer? Or in other words, in which geographic regions do we find the most contrail atmospheric conditions, and where are the most contrail forming flights?

A. Quantifying Contrails

Following the method described in section III, of a total of 873.442 flights analyzed, 40.441 (4.6%) were determined to satisfy both the SAC and ISSR conditions and are thus assumed to produce persistent contrails.

B. Temporal effects

In Fig. 4 the global occurrence of persistent contrail forming atmospheric conditions is shown per month. This value is a summation of the number of days per month of all of the 304 relevant stations. The red line indicates the total number of flights per month in the 50x50 km² polygons around each station. Fig. 5 shows the percentage of persistent contrail producing flights per month, with the total number of flights shown in the red line.

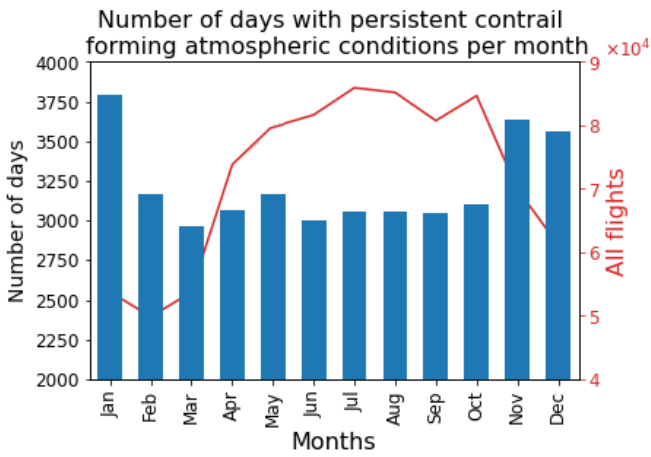


Figure 4: Monthly instances of persistent contrail atmospheric conditions in a bar chart, with the total number of flights per month as red line.

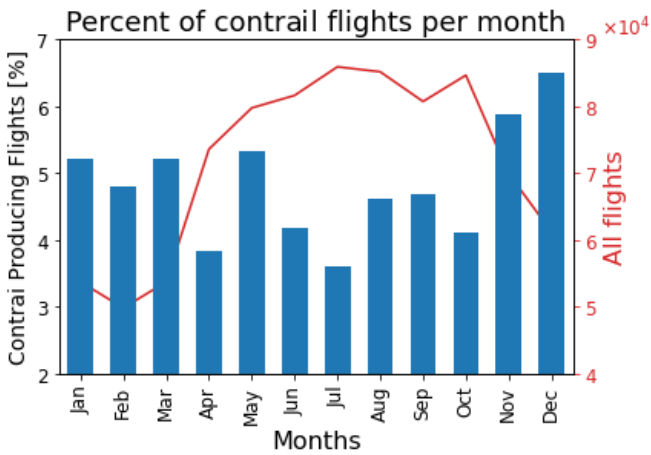


Figure 5: Monthly percentage of flights that produce persistent contrail in a bar chart, with the total number of flights per month as red line.

C. Geographical effects

In Fig. 6 (next page) a global yearly overview is shown of the occurrence of persistent contrail forming atmospheric conditions, namely instances of RH_i exceeding 100% and temperature falling below -40°C (233.15 K). The black dots indicate locations of stations and the shade and size of the circles indicate the number of instances when atmospheric conditions allow for formation of persistent contrails. The vertical and horizontal histograms indicate the latitudinal and longitudinal distribution of IGRA stations, respectively.

In Fig. 7 (next page) a similar graph is shown, however here the coloring of the circles indicate the percentage of aircraft that fly through these atmospheric conditions that allow for persistent contrail formation. The sizes of the circles indicate the number of the flights in absolute terms. The vertical and horizontal histograms display the latitudinal and longitudinal distribution of the total number of flights (in red) and the number of flights in these atmospheric conditions which allow

for formation of persistent contrails, respectively.

D. Altitude effects

In Fig. 8 the altitudes of persistent contrail forming atmospheric conditions and flight levels of all considered aircraft are shown.

Altitude distribution of aircraft and atmospheric regions

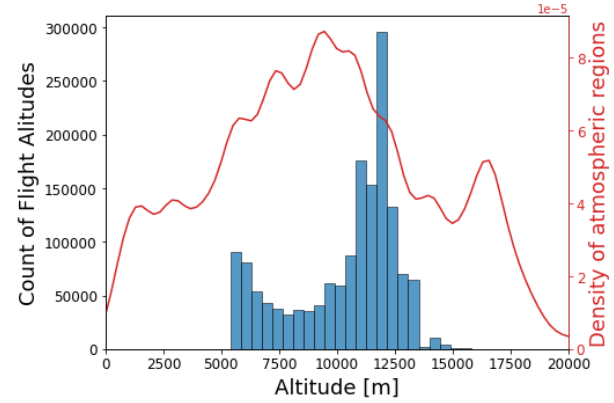


Figure 8: Flight altitudes of all considered aircraft and altitudes of persistent contrail forming atmospheric conditions

The opportunity to change flight level to stop contrail formation has been illustrated previously in Fig. 3. A histogram of the absolute nearest distance for a flight to 'exit' a persistent contrail forming atmospheric layer is shown in Fig. 9. From literature [6], we know that altitude changes of less than 1 km are feasible, and the histogram in Fig. 9 shows this is a significant portion (49%) of the flights.

Histogram of absolute altitude change necessary

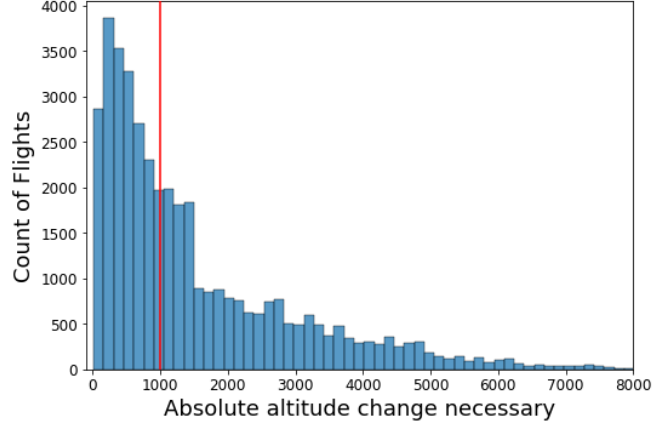


Figure 9: Histogram of all flight level changes (absolute values)

Filtering the histogram for deviations of less than 1 km, the absolute deviations are shown in Fig. 10, with negative values indicating a decrease and positive values indicating an increase of required altitude. A majority of the flights required an altitude decrease (63%), with the remaining 37% requiring an increase to exit the ISSR atmospheric region.

Global occurrence of persistent contrail forming atmospheric conditions

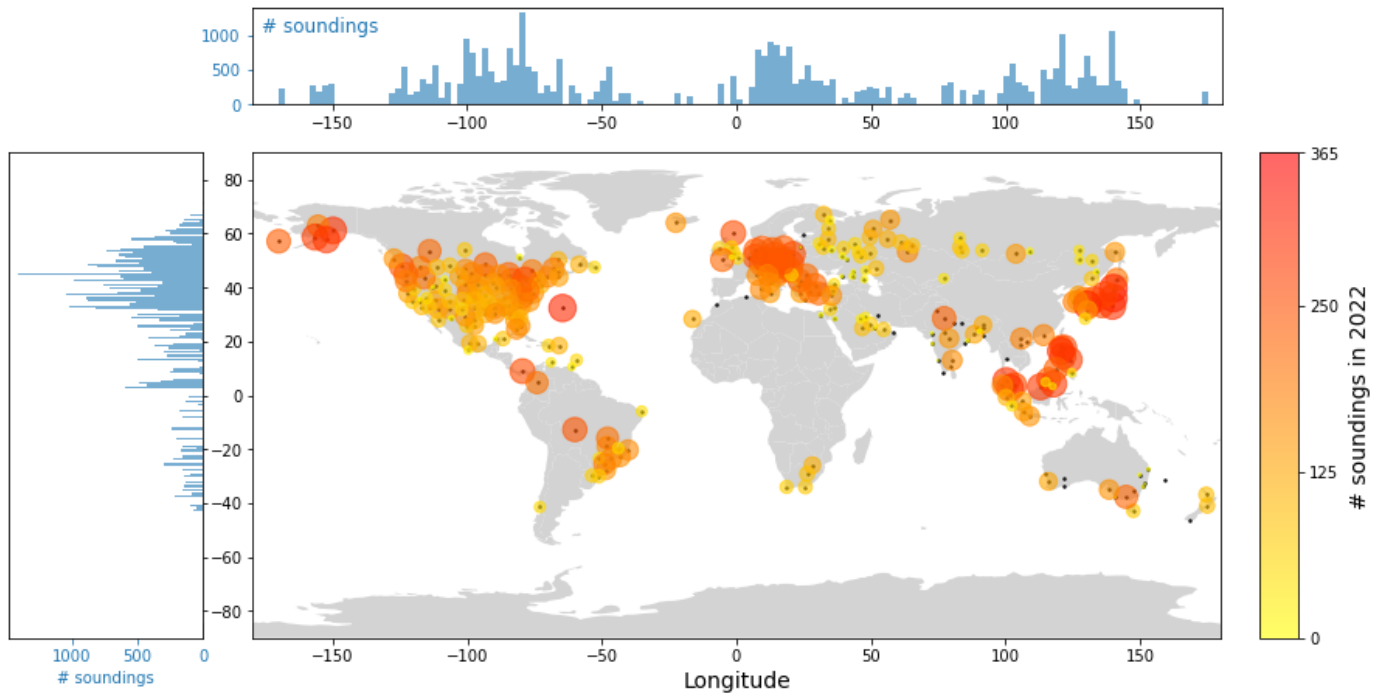


Figure 6: Global distribution of persistent contrail forming atmospheric conditions in the year 2022, with black dots indicating station location, and shaded circles indicating frequency of atmospheric conditions satisfying persistent contrail formation. The vertical and horizontal histograms indicate the latitudinal and longitudinal distribution of IGRA stations.

Percent of aircraft producing persistent contrails

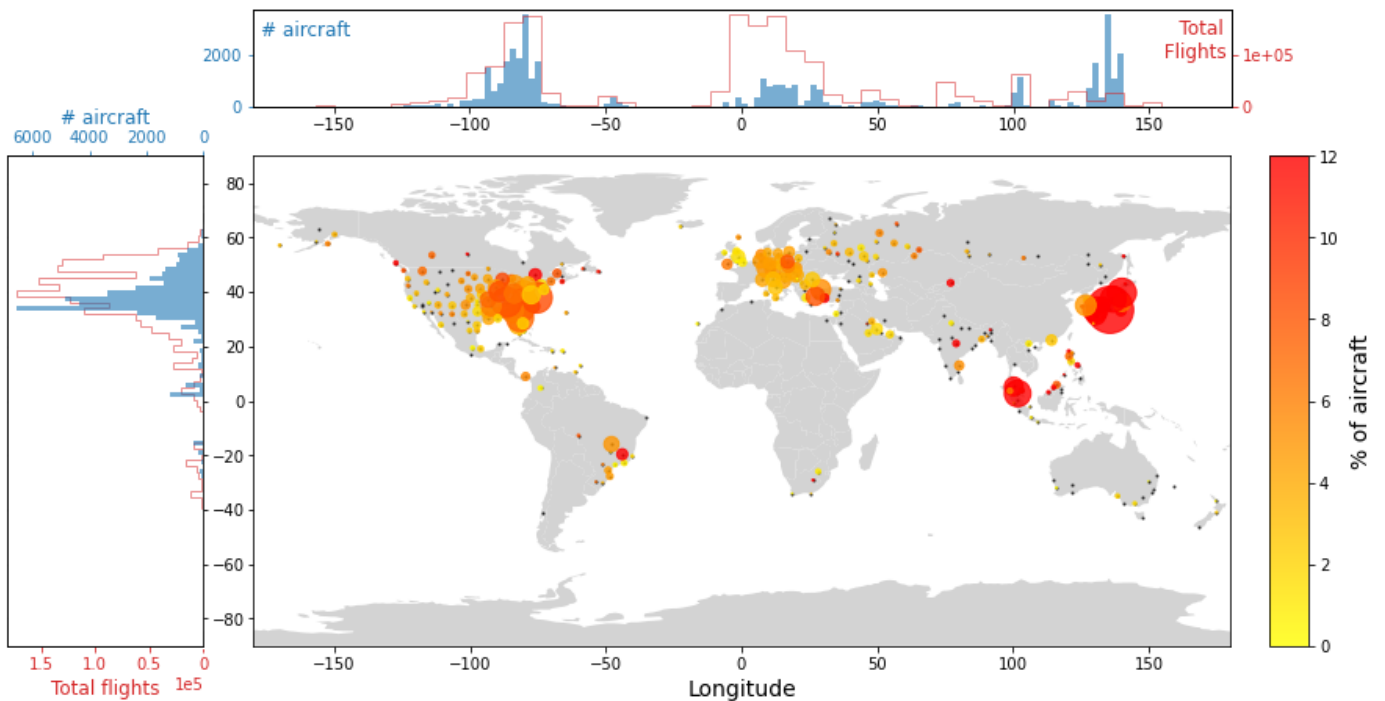


Figure 7: Percent of persistent contrail forming flights in the year 2022, with shading of the circles indicating the percent of total aircraft and the size of the circle indicating the absolute number of aircraft. The vertical and horizontal histograms indicate the latitudinal and longitudinal distribution of total flights (red) and persistent contrail forming flights (blue).

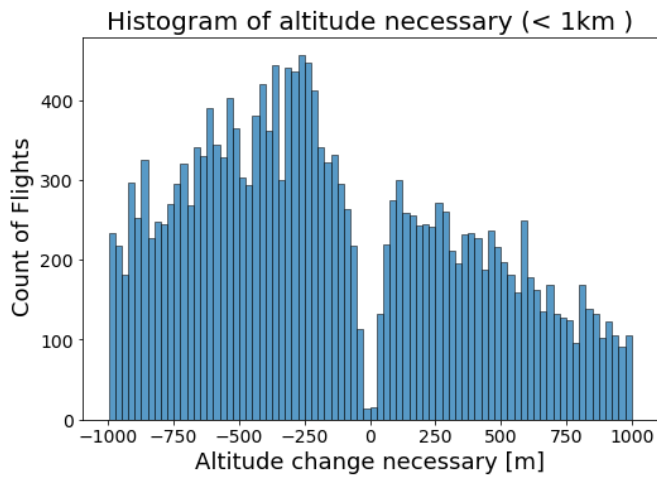


Figure 10: Histogram of flight level changes, less than 1 km, with negative values indicating a decrease and positive values indicating an increase of required altitude to avoid ISSR region.

In Fig. 11 we see the global distribution of these occurrences needing a flight level change of less than 1 km to stop contrail production. The shading of the circles indicates the percentage of total flights that are suitable for such an altitude change, and the size of the circle indicates the number of these flights. Fig. 12 (next page) shows a detailed look at some

regions of interest (Southeast Asia, Europe and U.S.A.).

Station locations with more than 10,000 yearly observed flights were selected, and sorted to show the top 25 stations with the smallest percentage of altitude diversions cause the largest percentage of contrails to be prevented. This is shown in Fig. 13 (next page).

V. DISCUSSION

In this section the structure of the results section is generally followed, in addition to a discussion on other aspects, such as data selection.

A. Data selection

The measurement series obtained by an ascending radiosonde is spread out over time, i.e. they are not simultaneous, as opposed to data from ECMWF which can be seen as an immediate snapshot of the atmosphere. From analysis of the data used in this paper, the typical recording time is around 1 hour. This time delay was mitigated by downloading the flight data from OpenSky within a time range of 1 hour before and after the launch of the weather balloon. In literature [20], it was established that ISSR's are slow moving atmospheric systems and so it is unlikely that the time delay between these two types measurements has a significant impact.

Based on atmospheric data gathered from the same source as [10], [6] estimates 15% of flights generate contrails in the United States, while our results indicate only 4.6%. Other research indicate a maximum of 34% of flights generate

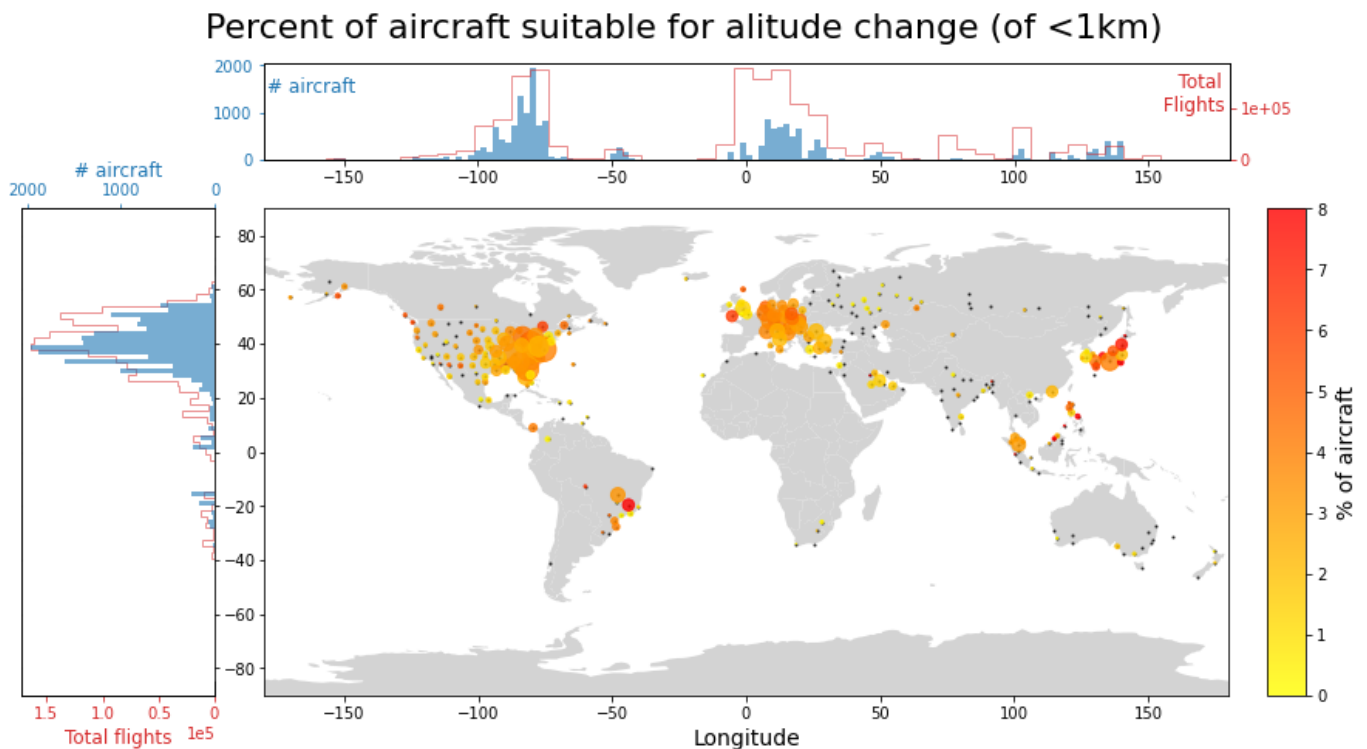


Figure 11: Percent of aircraft where an altitude change of less than 1 km would stop them producing contrails in the year 2022, with shading of the circles indicating the percent of aircraft and the size of the circle indicating the absolute number. The vertical and horizontal histograms indicate the latitudinal and longitudinal distribution of total flights (red) and aircraft suitable for an altitude change (blue).

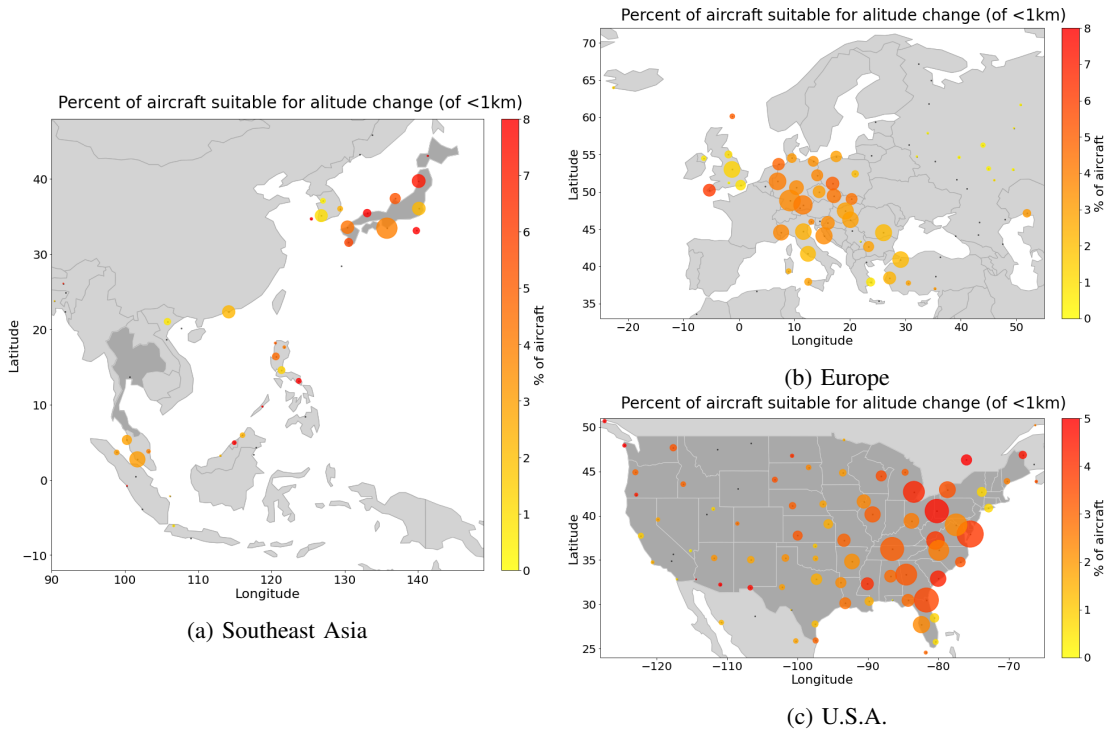


Figure 12: Detailed maps of percent of aircraft where an altitude change of less than 1 km would stop them producing contrails in the year 2022, with shading of the circles indicating the percent of aircraft and the size of the circle indicating the absolute number.

Top 25 Stations for contrail prevention

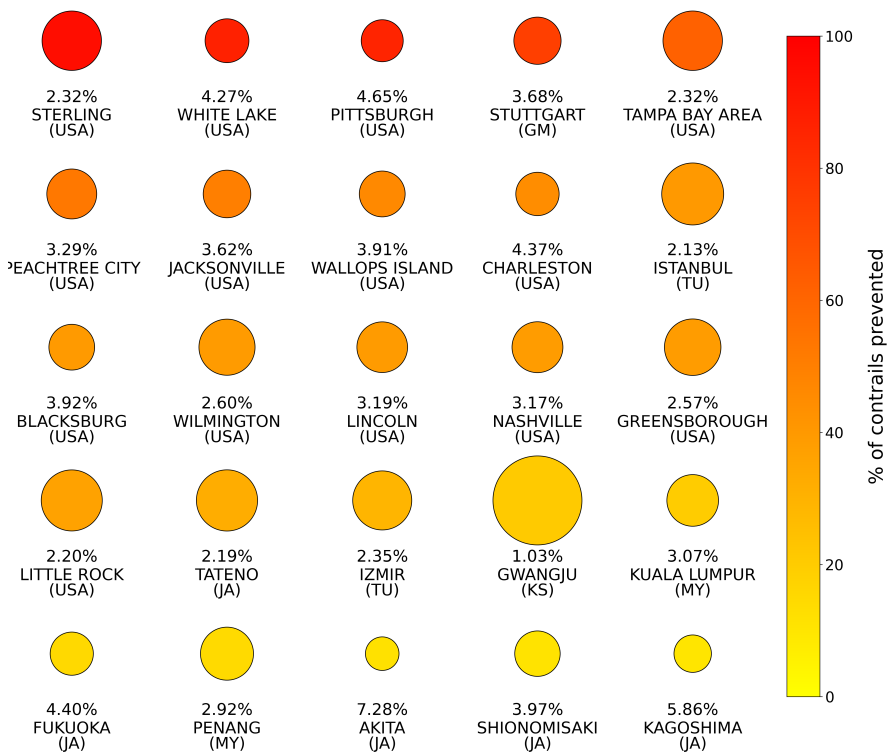


Figure 13: Top 25 stations, with more than 10,000 yearly flights. The circle color indicates the percent of contrails which are prevented, and the size of the circle the inverse of the number of flights which need to be diverted (percentage also shown below circles). Thus, large circles in dark red indicate that with a small number of altitude diversions, a large percentage of contrails can be prevented.

contrails on a given day [21], with the daily average percent of flights at 15.1% with a median of 13.8%. However, all three of these estimations also include mid-Atlantic flights, where ISSR's are very prevalent. OpenSky data has limitations regarding coverage over oceans, as can be seen in Fig. 1. This limited data coverage over oceans of both IGRA stations and OpenSky flight data are highly likely to be the reason for our underestimation of the overall percentage of contrail forming flights. Clearly it is worthwhile to analyze these ocean flights specifically using satellite networks [22], where the ocean coverage is more extensive. In particular, cross-Atlantic flights are considered to be highly suitable for altitude variations to minimize contrail formation [23].

B. Seasonal effects

Although air traffic peaks in the summer months, there is a higher occurrence of persistent contrails during winter, according to [23]. In Fig. 4 and 5, we see a similar result. While the total number of flights are lowest during the winter months, the number of days with persistent contrail forming atmospheric conditions and the percentage of contrail producing flights per month peak during the winter months (November, December and January). While the IGRA sounding data is global, the majority (87%) of the stations lie on the Northern Hemisphere (as can be seen in Fig. 11), and so we apply the Northern Hemisphere seasonal cycle to our analysis.

Importantly, [6] indicates that in their analysis the Summer months exhibited approximately three times higher Net Radiative Forcing than other months. Thus while the percentage of total contrail producing flights in the summer is lower, the climate impact of each individual flights is higher than a comparable winter flight. Considering the larger quantity of flights flown in the summer months, this indicates that more research is required to take these multiple effects into account in order to determine a climate-optimal system.

C. Geographical effects

The analysis of [6] focuses on contrail generation in the contiguous United States, and notes greater contrail prevalence in the south-eastern states. This is also visible in our results in Fig. 7. However, contrail formation in Pacific region of the U.S.A. is seemingly underestimated. In our previous research [10], a region over the Pacific Ocean (west of San Francisco) was identified as an area with an abundance of contrails. In satellite imagery, we see that these contrails form over the ocean, and are then blown to land by western winds. A likely explanation for the underestimation in this paper, is that the contrail forming atmospheric regions are mainly over the ocean, and so the ground station of IGRA do not measure these regions. This emphasises the importance of incorporating wind data into contrail prediction models. Linking IGRA to ECMWF data in these data space regions could provide a solution.

In [24], with geographical scope spanning the regions of Southern and Eastern Asia, they note the prevalence of contrail formation in Thailand and Japan. Our analysis confirms this finding, as seen in Fig. 6. With the high growth rates of air

traffic in south-eastern Asia, these will become increasingly relevant with regards to contrail mitigation.

Meanwhile, the main driver of contrail prevalence in Europe appears to be the large quantity of flights, rather than the (relatively low) high percentage of contrail producing flights. Nonetheless, the occurrence of atmospheric conditions allowing for contrail formation are relatively high, see Fig. 6. Perhaps the flight altitudes flown in Europe could already be beneficial for minimizing contrail formation or that contrail forming atmospheric regions are thinner and thus less likely to at a selected flight altitude, more research would be required to answer these questions.

Regrettably, large swaths of Africa and South-America have little to no OpenSky coverage (see Fig. 1). Once again, data from satellite networks could be used to minimize these data gaps.

D. Quantification of altitude changes

The altitude changes necessary to 'exit' persistent contrail forming atmospheric conditions shown in this paper are most likely an underestimation of a few hundred meters. This is because the distance is calculated to the nearest measurement point, even though through interpolation suitable atmospheric conditions could occur at a nearer altitude.

In our analysis, the aircraft has the option to either increase or decrease the altitude to 'exit' the atmospheric layer. In Fig. 10 a histogram of the necessary flight level deviation is shown. In a majority (63%) of these flight alterations, the nearest option is reached by decreasing the altitude. However, generally, altitude decreases are unfavourable when minimizing climate impact, since it decreases the fuel efficiency. More research regarding the trade-off of the contrail climate effects and the additional fuel burn would be necessary to determine which altitude would be the most climate-optimal in this scenario.

In Fig. 11 we see that the main geographical regions where contrails could be minimized, within the operations of today's aircraft, are: mid-western Europe (detail in Fig. 12b), south-eastern United States (Fig. 12c) and Southeast Asia (Fig. 12a). In one station in Sapporo, Japan (a city on the northern island of Hokkaido), 15% of yearly flights are suitable for an altitude change of less than 1 km to minimize contrails. Visual verification of 10 stations with these high percentages was done using MODIS True Color images, which confirmed the presence of an abundance on contrails at these locations.

In mid-western Europe we also see large number of suitable flights, reinforcing the idea presented in subsection V-C that atmospheric regions allowing for contrail formation are thinner and thus require smaller altitude deviations.

Fig. 13 identifies regions where a relatively small operational intervention can make a large climate impact. The U.S.A., Europe and Japan emerge as regions where the highest percentage of contrails can be prevented by an altitude change of less than 1 km. For example at one station in Sterling, Virginia (U.S.A.), 2.3% of yearly flights could be diverted to prevent 94% of contrails. This emphasises the importance of contrail prediction modeling, to identify these atmospheric conditions and flights.

VI. CONCLUSION

In this paper, global contrail formation was assessed using open flight and weather balloon data of the year 2022. Furthermore, the magnitude of altitude changes necessary to minimize contrail formation was quantified. Linking these datasets, the flights which are predicted to produce persistent contrails are identified, as both flying at an altitude where atmospheric conditions satisfy the Schmidt-Appleman Criterion and ISSR (ice-supersaturation region) conditions.

Analysis of these persistent contrail flights show that there are strong geographical and seasonal influences for identifying contrail forming flights. Besides this, our paper identifies regions where relatively small operational interventions can make a large climate impact, emphasizing the importance of contrail prediction modeling, to identify these atmospheric conditions and flights.

The climate impact of contrails is also dependent on geographical and seasonal variations. Considering the aim is to maximize overall climate gains, further quantification of individual contrail climate impact is necessary to determine whether to focus upon areas with few flights but with persistent contrails having a large climate impact, or areas with larger number of flights where persistent contrails have little climate impact, or finding a compromise between these two.

The importance of wind effects in contrail prediction is seen in the underestimation of contrail occurrence in the western United States. In combination with the climate impact of each individual contrail differing seasonally, these multiple effects need to be taken into account in order to determine a climate-optimal system.

It is believed that hydrogen power will be a potential solution to aviation's CO₂ emissions, however minimizing the climate impact caused by contrails remains unresolved, even for hydrogen flight. Eventually, for a climate-optimized routing model, characteristics, such as persistence, warming/cooling, energy forcing, related to contrail formation will need to be predicted based on atmospheric conditions, and can be directly implemented for hydrogen flight as well.

This paper contributes to the understanding of the scale of the contrail question, and where and when the biggest climate gains can be achieved. This allows us to determine which data to train the model on and where to place our research emphasis.

REFERENCES

- [1] D. Lee, "The contribution of global aviation to anthropogenic climate forcing for 2000 to 2018." *Atmospheric Environment*, vol. 244, 2021.
- [2] U. Schumann, K. Graf, and H. Mannstein, "Potential to reduce the climate impact of aviation by flight level changes." *3rd AIAA Atmospheric Space Environments Conference*, 2011.
- [3] U. Schumann, "On conditions for contrail formation from aircraft exhausts." *Meteorol. Zeitschrift*, vol. 4-23, 1996.
- [4] P. Ferris, "The formation and forecasting of condensation trails behind modern aircraft." *Meteorological Applications*, vol. 3, 2007.
- [5] B. Kärcher, "Formation and radiative forcing of contrail cirrus." *Nat. Commun.*, vol. 9, 2018.
- [6] D. Avila, L. Sherry, and T. Thompson, "Reducing global warming by airline contrail avoidance: A case study of annual benefits for the contiguous united states." *Transportation Research Interdisciplinary Perspectives*, vol. 2, 2019.
- [7] B. Sridhar, H. Ng, F. Linke, and N. Chen, "Benefits analysis of wind-optimal operations for transatlantic flights," *14th AIAA Aviation Technology, Integration, and Operations Conference*, 2014.
- [8] H. Gao and R. J. Hansman, "Aircraft cruise phase altitude optimization considering contrail avoidance." *Master's Thesis, Department of Aeronautics, Massachusetts Institute of Technology. Report No. ICAT-2013-10.*, 2013.
- [9] J. Rosenow and T. S. M. Fricke, H. and Luchkova, "Minimizing contrail formation by rerouting around dynamic ice-supersaturated regions." *Aeronautics and Aerospace Open Access Journal* 2, vol. 3, 2018.
- [10] E. Roosenbrand, J. Sun, and J. Hoekstra, "Examining contrail formation models with open flight and remote sensing data." *SIDS 2022*.
- [11] E. Roosenbrand, J. Sun, I. Dedoussi, D. Stam, and J. Hoekstra, "Assessing and modelling climate optimal flights using open surveillance and remote sensing data." *ICRAT 2022*.
- [12] I. Durre, X. Yin, R. Vose, S. Appellequist, and J. Arnfield, "Enhancing the data coverage in the integrated global radiosonde archive," *Journal of Atmospheric and Oceanic Technology*, vol. 35, 2018.
- [13] J. Nash, "Measurement of upper-air pressure, temperature and humidity." *Instruments and Observing Methods*, vol. 121, 2015.
- [14] I. Durre, R. Vose, and D. Wuerz, "Overview of the integrated global radiosonde archive," *Atmospheric Environment*, vol. 244, 2021.
- [15] M. Strohmeier, O. Xavier, L. Jannis, M. Schäfer, and V. Lenders, "Crowdsourced air traffic data from the opensky network 2019–2020." *Journal of Air Transport Management*, vol. 94, 2022.
- [16] J. Sun, L. Basora, X. Olive, M. Strohmeier, M. Schafer, I. Martinovic, and V. Lenders, "Opensky report 2022: Evaluating aviation emissions using crowdsourced open flight data," *AIAA/IEEE Digital Avionics Systems Conference - Proceedings*, vol. 94, 2022.
- [17] D. Sonntag, "Advancements in the field of hygrometry." *Meteorologische Zeitschrift*, vol. 3, 1994.
- [18] S. Buehler and N. Courcoux, "The impact of temperature errors on perceived humidity supersaturation." *GEOPHYSICAL RESEARCH LETTERS*, vol. 30, 2003.
- [19] S. Gillies *et al.*, "Shapely: manipulation and analysis of geometric objects," [toblerity.org](https://github.com/Toblerity/Shapely), 2007–. [Online]. Available: <https://github.com/Toblerity/Shapely>
- [20] D. Avila, "Methodology for contrail inventory analysis," *Dissertation*, vol. George Mason University, 2010.
- [21] L. Avila, D. and Sherry, "A contrail inventory of u.s. airspace (2015)," *Proceedings IEEE Integrated Communications, Navigation and Surveillance (I-CNS) Conference 2019*, vol. 9, 2019.
- [22] J. Cappaert, "The spire small satellite network." *Handbook of Small Satellites: Technology, Design, Manufacture, Applications, Economics and Regulation*, vol. 1-21, 2020.
- [23] R. Teoh, U. Schumann, E. Gryspeerd, M. Shapiro, J. Molloy *et al.*, "Aviation contrail climate effects in the north atlantic from 2016 to 2021," *Atmos. Chem. Phys.*, vol. 22, 2022.
- [24] R. Meyer, R. Buell, C. Leiter, H. Mannstein, S. Pechtl, T. Oki, and P. Wendling, "Contrail observations over southern and eastern asia in noaa/avhrr data and comparisons to contrail simulations in a gcm," *International Journal of Remote Sensing*, vol. 28, no. 9, pp. 2049–2069, 2007.